Droplet microemulsions at the emulsification boundary: The influence of the surfactant structure on the elastic constants of the amphiphillic film

M. Gradzielski, D. Langevin, T. Sottmann, and R. Strey

Articles you may be interested in

Droplet microemulsions at the emulsification boundary: The influence of the surfactant structure on the elastic constants of the amphiphillic film

M. Gradzielski
Lehrstuhl für Physikalische Chemie I, Universität Bayreuth, D-95440 Bayreuth, Germany

D. Langevin
Centre de Recherche Paul Pascal, Avenue Schweitzer, F-33600 Pessac, France

T. Sottmann
Max-Planck Institut für Biophysikalische Chemie, Postfach 2841, D-37018 Göttingen, Germany

R. Strey
Institut für Physikalische Chemie Köln, Luxemburger Str. 116, D-50939 Köln, Germany

The droplet structure of nonionic oil/water (O/W) microemulsions has been investigated by small-angle neutron scattering (SANS). The sum $2\kappa + \overline{\kappa}$ of the elastic moduli that can be deduced from the experimental polydispersity compares well with the values independently deduced from interfacial tension measurements, thereby showing that our determination of the elastic constants appears to be reliable. In this study, nonionic surfactants of different chain length and with different head groups were investigated (polyethylene glycol monoalkylether C_iE_j and alkyldimethlyamine oxides). The interpretation of the experiment data shows that the elasticity of the amphiphilic film increases with the thickness of the amphiphilic film. However, it does not depend significantly on the type of the head group but is primarily determined by the length of the alkyl chains of the surfactant. In mixtures of surfactants of different chain lengths, the sum $2\kappa + \overline{k}$ is found to vary linearly with the molar composition of the mixture. © *1997 American Institute of Physics.* [S0021-9606(97)50719-7]

I. INTRODUCTION

The elastic properties of amphiphilic films, as they are typically formed in self-assembling structures, are an important factor in understanding their properties. The knowledge of the elastic constants allows for a description of phase behavior and structures that are present in the corresponding systems.[1–3] A very simple system in that context is microemulsions, since, because of their low interfacial tensions, the leading term in the free energy should be given by the bending energy,[4] which can be described in terms of two elastic constants, the mean bending modulus κ, and the Gaussian modulus $\overline{k}$ (Ref. 5)

Microemulsions occur in a variety of structures, the most prominent of which are: oil-in-water (O/W) droplets, water-in-oil (W/O) droplets, and bicontinuous structures. In all cases they contain a surfactant monolayer that separates the hydrophilic microdomains from the hydrophobic microdomains. For the case of droplet structures, the situation becomes particularly simple for the theoretical description.[5,6] Therefore, we chose to investigate O/W microemulsions and to deduce from these studies values for the elastic constants of the corresponding amphiphilic films.

Similar studies, using the same approach to deduce the elastic constants from scattering experiments and interfacial tension measurements, have been done before.[7–11] The aim of the present study was to vary systematically the molecular structure of the surfactants that make up the amphiphilic film in order to see how its structure is related to the elasticity of the film. In particular, we varied the chain length of the sur-

factant (and thereby the thickness of the amphiphilic film) in order to see how it influences the rigidity of the corresponding amphiphilic film. This should enable one to understand the elastic properties of the amphiphilic film in terms of the molecular composition of the given system. Such knowledge should be very helpful in understanding the properties of surfactant systems, and in particular the changes in phase behavior that occur upon changing the surfactant length, as well as the properties of the corresponding aggregates that are formed by these surfactants.

II. EXPERIMENTAL METHODS

A. Small-angle neutron scattering (SANS)

The SANS experiments on the C_iE_j systems were carried out on the PAXE instrument of the Laboratoire Léon Brillouin, Laboratoire Commun CEA–CNRS, Saclay, France. The wavelength chosen was 6 Å and sample-to-detector distances of 1.15 and 5.05 m were employed. Thereby a q-range of 0.0068–0.31 Å has been covered in the experiments. The SANS measurements on the amine oxide systems were performed on the D11 instrument of the Institut Laue–Langevin, Grenoble, France. Here different conditions were chosen, but always in such a way that the characteristic minimum in the scattering curves was well covered by the chosen q-range.

All samples were investigated close to the emulsification boundary, i.e., saturated with the hydrocarbon to be solubilized. This was achieved by measuring the corresponding

samples of the C_iE_j surfactants about 0.5 K above the emulsification boundary. It has been shown before that so close to the phase boundary the observed scattering curves are practically identical to those of samples in the two-phase equilibrium.[8] For the case of the amine oxide system, a small amount of excess oil was always present to ensure that the system was saturated with oil. The presence of a small amount of excess oil should not influence the composition of the system because of the rather low monomeric solubility of the surfactants in oil.

The scattered intensity was recorded on a 2D detector and the data were radially averaged afterwards. This set of data was corrected for the efficiency of the detector (by means of comparison with the spectrum of water) and then converted into the differential cross section by means of standard procedures.[2]

B. Interfacial tension measurement

The ultra-low interfacial tensions were measured using a Krüss SITE 04 spinning-drop tensiometer. This type of tensiometer, developed by Cayias *et al.*,[13] and subsequently modified by Burkowsky and Marx,[14] permits the measurement of interfacial tensions down to 10^{-4} mN/m. It consists of a thermostatable horizontal glass capillary rotating about its long axis with a maximum speed of 10 000 rpm.

After phase separation, the oil-phase (b) was injected into the rotating capillary filled with the aqueous phase (a) in order to measure the interfacial tension between these two phases γ_{ab}. The interfacial tensions were calculated according to a relation derived by Vonnegut.[15] He considered the drop as a cylinder of radius r and length l with hemispherical ends. For $l > 8r$, the interfacial tension γ_{ab} is given by

$$\gamma_{ab} = \tfrac{1}{4}(\rho_a - \rho_b) \cdot \omega^2 \cdot r^3, \tag{1}$$

where ω is the angular velocity and $(\rho_a - \rho_b)$ is the density difference of the two phases. A more detailed description of the interfacial tension measurements with the spinning-drop technique is given elsewhere.[16]

All interfacial tensions have been measured using hydrogenated decane instead of the deuterated decane as used in the SANS experiments. However, the isotopic substitution should not influence the interfacial tension measurements, since phase behavior and properties of O/W microemulsions are typically only very slightly affected by the isotopic substitution. However, the use of D_2O instead of H_2O typically induces a phase shift by about 2K,[17] which had been accounted for in the experiments.

III. MATERIALS

D_2O (degree of deuteration $> 99.9\%$) and deuterated n-D_{18}-octane (isotopic purity: 99%) were from Cambridge Isotope Laboratory (Cambridge, MA). n-D_{22}-decane (isotopic purity: 99%) was from Euriso-top Groupe C. E. Saclay (Gif-sur-Yvette, France). Triethylenegylcol mono-octylether (C_8E_3), pentaethyleneglycol monooctylether (C_8E_5), tetraethylenegylcol monodecylether ($C_{10}E_4$), pentaethyleneglycol monodecylether ($C_{10}E_5$), and hexaethyleneglycol mono-

TABLE I. Composition of the samples of the O/W microemulsions composed of the nonionic C_iE_j surfactants with D_{18}-octane. α is the weight percentage of oil in the mixture of oil and water, c the weight percentage of the surfactant in the system, Φ_o and Φ_s the corresponding volume fractions, and T_l and T_u the temperatures of the lower and upper phase boundary of the one-phase region.

Surfactant	α	c	Φ_o	Φ_s	T_l in °C	T_u in °C
C_8E_3	1.54	1.77	0.0204	0.0204	5.0	8.8
$C_{10}E_4$	1.59	1.92	0.0211	0.0219	9.0	16.2
$C_{12}E_5$	1.49	1.77	0.0197	0.0201	17.8	23.6
$C_{10}E_5$	1.54	1.82	0.0204	0.0205	30.0	35.8
$C_{10}E_6$	1.54	1.86	0.0204	0.0207	45.6	51.4
C_8E_5	1.26	1.98	0.0166	0.0219	47.8	50.6

decylether ($C_{10}E_6$) were purchased from Fluka (Neu Ulm, Germany) with a purity $> 98\%$. Pentaethyleneglycol monododeclyether ($C_{12}E_5$) was obtained from Nikko (Tokyo, Japan) with a purity $> 98\%$. The cloud points at critical composition of the binary system's water–C_iE_j were checked in order to verify the purity and to monitor possible degradation.[18] All solvents were used without further purification.

The compositions are given by the oil/(water+oil) weight fraction α and the surfactant weight fraction γ, and are summarized in Table I, together with the lower and upper temperature for the one-phase microemulsion regime. For the calculation of the volume fractions Φ_i, we assumed ideal mixing using the known densities given in g/cm^3 at 20 °C for D_2O (1.105), D-octane (0.814), C_9E_3 (0.948), C_9E_5 (0.985), $C_{10}E_4$ (0.959), $C_{10}E_5$ (0.973), $C_{10}E_5$ (0.987), and $C_{12}E_5$ (0.967).

The sample compositions are given in Table I. In all cases we tried to have as close as possible equal volume fractions of oil and surfactant (in order to have microemulsion droplets of similar size). The total volume fraction, i.e., surfactant plus oil, of the dispersed phase was around 4%. This means that the droplet phase can be considered to be dilute.

The amine oxides (dodecyldimethylamine oxide $C_{12}DMAO$, tetradecyldimethylamine oxide $C_{14}DMAO$, hexadecyldimethylamine oxide $C_{16}DMAO$, oleyldimethylamine oxide ODMAO) were gifts from Hoechst, Gendorf (Germany), and were recrystallized twice from acetone. All samples were saturated with D_{22}-decane and the volume fraction of all samples was about 3.5% (for surfactant plus decane). For the calculation of the volume fraction, the density of 0.843 g/cm^3 for D_{22}-decane and 0.891 g/cm^3 for the amine oxides was employed here.

IV. THEORETICAL BACKGROUND

A. Theory of microemulsion droplets

Structures and properties of microemulsions can be rationalized via the description of the amphiphilic film in terms of the elastic constants.[4] In general, the elastic free energy of an amphiphilic film can be described by the following expression:[19,20]
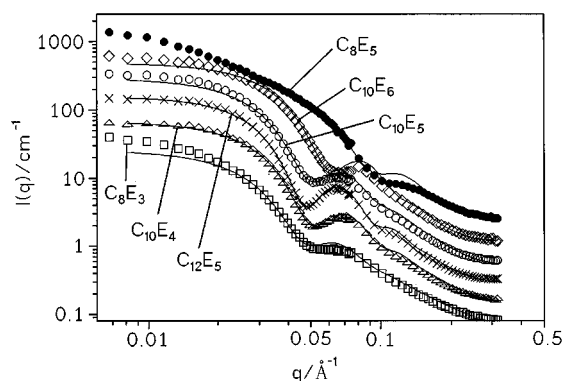
FIG. 1. Scattering curves for O/W microemulsions of type O_iE_j/D_{18}-octane/D_2O for various surfactants. All samples were close to the two-phase equilibrium and measured at the temperatures given in Table II. □: C_8E_3; △: $C_{10}E_3$; x: $C_{12}E_5$; ○: $C_{10}E_5$; ◇: $C_{10}E_5$; ●; C_9E_5 (the absolute units are valid for C_8E_3, subsequent samples are each multiplied by a factor of 2 for better lucidity). The fitted curves are given as solid lines.

$$F = \int d\,A[(c_1 + c_2 - 2 \cdot c_0)^2 \cdot (\kappa/2) - c_1 \cdot c_2 \cdot \bar{\kappa}] + N \cdot k \cdot T \cdot f(\Phi), \tag{2}$$

where κ is the mean bending modulus, $\bar{\kappa}$ the Gaussian modulus, c_0 the spontaneous curvature, c_1 and c_2 the principal curvatures of the amphiphilic film, and $f(\Phi)$ a concentration dependent term that takes into account the entropy of mixing. For $f(\Phi)$ we always used the random mixing approximation, as it has been shown before to be a good description of the entropic contribution for such systems:[8,21]

$$f(\Phi) = (1/\Phi) \cdot \{\Phi \cdot \ln \Phi + (1-\Phi) \cdot \ln(1-\Phi)\}. \tag{3}$$

In particular the case of microemulsion droplets has been treated in some detail,[5,6] and here structural properties as well as the macroscopic interfacial tension can be described by means of the elastic constants.

If one considers the thermodynamically particularly simple case of microemulsion droplets saturated with the solubilizate, relatively simple relations between the elastic constants and the polydispersity index p and the interfacial tension γ have been derived.[8,21–23] For the polydispersity index p, one obtains

$$p^2 = \frac{\langle R^2 \rangle}{\langle R \rangle^2} - 1 = \frac{k \cdot T}{8 \cdot \pi \cdot (2\kappa + \bar{\kappa}) + 2 \cdot k \cdot T \cdot f(\Phi)} \tag{4}$$

and the macroscopic interfacial tension can be written as

$$\gamma = \frac{2\kappa + \bar{\kappa}}{R_m^2} + \frac{k \cdot T}{4 \cdot \pi \cdot R_m^2} f(\Phi). \tag{5}$$

Therefore it is evident that if one determines the polydispersity index p experimentally, one can directly relate it via Eq. (4) to the sum $2\kappa + \bar{\kappa}$ of the elastic constants. In addition, one can determine independently $2\kappa + \bar{\kappa}$ from Eq. (5), with the measured interfacial tension γ, together with the mean radius R_m of the droplets. This means that two completely unrelated experimental methods, measurement of the interfacial tension and a small-angle scattering experiment, allow for two independent ways to deduce $2\kappa + \bar{\kappa}$ from experimental data.

Furthermore, one is able to eliminate the entropic term from Eqs. (4) and (5) and thereby obtain an expression that interrelates all three experimentally accessible quantities R_m, p, and γ (see Ref. 8):

$$W = 8\pi \cdot p^2 \cdot R_m^2 \cdot \gamma = k \cdot T. \tag{6}$$

This relation now allows for a prediction of one of the three quantities if the two other ones are known, i.e., there exists a clear relation between these experimental quantities.

B. Scattering theory

All scattering experiments were carried out in the shell contrast, i.e., both the solvent (water) and the hydrocarbon were used in their fully deuterated form. This means that the only remaining hydrogenated compound is the surfactant, and therefore one observes exclusively the scattering due to the amphiphilic film. This contrast condition is particularly suited for our experiments since it is more sensitive than the bulk contrast for the determination of the polydispersity index, which is a key quantity in our analysis. Relatively low polydispersities show up in the scattering curves as a minimum around $q = \pi/R$, which is more pronounced the lower the polydispersity index p.

This means that we should be able to describe our experimental scattering curves with a model of polydisperse spherical shells. Here two principally different models may be employed, which differ with respect to the way the scattering length density varies at the interface of the amphiphilic film:

(i) sharp boundaries, i.e., a step profile of the scattering length density (model 1);
(ii) diffuse boundaries that are described by a Gaussian profile of the scattering length density (model 2).

The form factor $P(q)$ that arises for the two different models has been discussed in some detail before.[24] It should be noted, that although both models will differ somewhat in how well they describe the minimum (due to the relatively low polydispersity of the corresponding droplets), and in particular the high q part of the scattering curve, they yield very similar values for the polydispersity index p if fitted to experimental data.[24] This means that the detailed structure of the amphiphilic shell does not influence the outcome of our analysis to a significant degree, since in the following we only use this value p for the determination of the elastic moduli.

With the given form factor $P(q)$, the scattering intensity of a microemulsion droplet system can be calculated by

$$l(q) = {}^1N \int d\,r \cdot h(r) \cdot P(q,r) \cdot S(q), \tag{7}$$

where ${}^1N$ is the number density of the aggregates, $h(r)$ the distribution function for the radii [chosen to be a Schulz function for model 1 and to be a Gaussian function for model
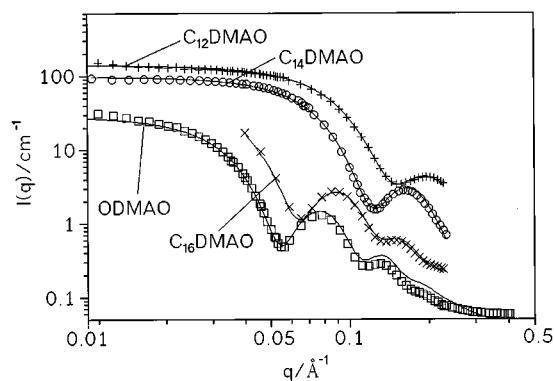
FIG. 2. Scattering curves for O/W microemulsions of the type C_nDMAO/D_{22}-decane/D_2O measured at 25 °C (for C_{16}DMAO at 30 °C). +: C_{12}DMAO; ○: C_{14}DMAO; ×: C_{16}DMAO; □: ODMAO (the absolute units are valid for ODMAO, subsequent samples are each multiplied by a factor of 3 for better lucidity). The fitted curves are given as solid lines.

2 (for the reason of simpler calculation, i.e., for a Gaussian distribution an analytic solution exists)],[24] and $S(q)$ the interparticle structure factor. For $S(q)$ a simple hard-sphere model[25] was employed where the hard-sphere radius was fixed to be the mean value of that of the form factor. However, since all samples investigated only had fairly low volume fractions, the particular choice of $S(q)$ has only a very minor influence on the outcome of the fitting procedure.

For the analysis of the scattering data, both models were always fitted to the experimental data, while taking into account the experimental wavelength distribution of $\Delta\lambda/\lambda = 0.1$ (FWHM). Here the absolute intensities were used and the fitting procedure employed in such a way as to minimize to the logarithm of the mean-square deviation.

V. RESULTS AND DISCUSSION

A. Alkyl poly glycol ethers C_1E_1

As discussed above, one way to access the sum $2\kappa + \bar{\kappa}$ of the bending constants is via the determination of the polydispersity index p of the corresponding microemulsion droplets [cf. Eq. (4)]. This can be done by means of SANS measurements in the shell contrast, which is particularly susceptible to the polydispersity of the droplets. Therefore, a series of oil-in-water (O/W) microemulsions was investigated, where the chain lengths of both the alkyl chain and the hydrophilic EO groups were systematically varied, in order to study their influence on the polydispersity index. The samples were chosen in such a way as to have a common radius of ~50 Å and also to have similar interfacial tension. This could be done by properly choosing the temperature for the given system. The corresponding temperatures and the composition of the systems are summarized in Table I. All the samples were close to the emulsification boundary and contained a volume fraction of ~4%.

The obtained scattering curves are given in Fig. 1 and were analyzed with the two models for the scattering of shell structures discussed in Sec. IV B. For all samples the model of the diffuse shell boundaries yields the better fits. The re-

TABLE II. O/W microemulsions with various polyethyleneglycol monoalkyl ether (C_iE_j) surfactants (always with D_{18}-octane). Given are the measuring temperature T, mean radius R_m, thickness parameter t, polydispersity index p and the sum $2\kappa + \bar{\kappa}$ (deduced from p), interfacial tension γ and the sum $2\kappa + \bar{\kappa}$ (deduced from γ), and the factor W as defined by Eq. (6).

Surfactant	C_8E_3	$C_{10}E_4$	$C_{12}E_5$	$C_{10}E_5$	$C_{10}E_6$	C_8E_5
T in °C	5.8	9.4	17.9	30.6	46.1	48.3
R_m in Å	57.7	57.2	58.6	57.2	47.3	29.1
t in Å	3.41	4.92	5.69	5.32	6.24	5.00
p	0.213	0.145	0.113	0.164	0.153	0.236
$(2\kappa + \bar{\kappa})/kT$	1.21	2.24	3.46	1.81	2.04	1.05
γ in mN/m	0.134	0.199	0.220	0.162	0.227	0.256
$(2\kappa + \bar{\kappa})/kT$	1.42	1.94	2.38	1.53	1.42	0.76
W/kT	1.32	0.88	0.61	0.85	0.68	0.68

sults are given in Table II. This is reasonable since one can expect the EO head groups of the surfactant molecules to protrude quite largely into the aqueous (D_2O) boundaries of the microemulsion droplets, thereby forming a diffuse layer around the droplet. In addition, the alkyl part of the surfactant will be penetrated by the (deuterated) hydrocarbon, and both effects will render the variation of the scattering length density less abrupt and more like a Gaussian distribution.

The corresponding fit curves are also given in Fig. 1 as solid lines. In all cases, except that of C_8E_5, they show very good agreement with the experimental data. For C_8E_5 one observes deviations in the low q range, where the experimental intensity is significantly larger than expected from theory for spherical particles. However, this deviation can be explained by the fact that this system was very close to the lower critical line. [It should be noted here that the temperature T_l in Table I denotes the point below which the microemulsion starts to expel excess oil (emulsification failure), and T_u is the critical temperature above which a surfactant-rich phase is formed, i.e., here a critical point is reached]. Therefore, here one already observes a contribution of the critical scattering due to the proximity of this critical point[26] (whereas no such scattering is to be expected close to T_l). This contribution may be accounted for by an Ornstein–Zernike type of expression for the structure factor $S(q)$ as has been shown in similar experiments.[27,28]

TABLE III. Experiment parameters for O/W microemulsions of alkyl amine oxides with decane. Given are the mean radius R_m, shell thickness d, polydispersity index p, and the sum $2\kappa + \bar{\kappa}$ (deduced from p), interfacial tension γ and the sum $2\kappa + \bar{\kappa}$ (deduced from γ), and the factor W as defined by Eq. (6).

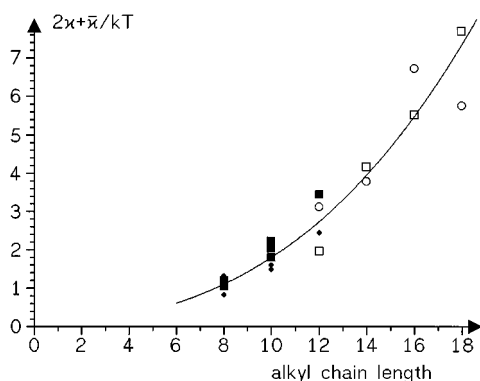| Surfactant	C_{12}DMAO	C_{14}DMAO	C_{16}DMAO	OleylDMAO
R_m in Å	19.5	23.8	46.8	54.9
d in Å	10.8	15.1	11.8	13.5
p	0.156	0.102	0.088	0.073
$(2\kappa + \bar{\kappa})/kT$	1.98	4.18	5.53	7.71
γ in mN/m	3.11	2.53	1.20	0.73
$(2\kappa + \bar{\kappa})/kT$	3.13	3.80	6.74	5.77
W/kT	1.76	0.91	1.24	0.72

FIG. 3. The sum $2\kappa + \bar{\kappa}$ as a function of the alkyl chain length i for the various surfactants. Solid symbols: polethylenegylcol alkyl ethers C_iE_j; open symbols: amine oxides. □ ■: deduced from the polydispersity index p_i ○ ●: deduced from the interfacial tension γ.

FIG. 4. Scattering curves for O/W microemulsions with surfactant mixtures of $C_{12}E_5$ and C_8E_3 (hydrocarbon: D_{22}-decane) at 10 °C. Molar content of C_8E_3: □: 0%; △: 32.4%; ×: 52.3%; ◇: 68.9%; +: 86.6%; ○: 100% (absolute units are valid for 0% C_8E_3, subsequent samples are each multiplied by a factor of 2 for better lucidity, in the case of 100% C_8E_3 by a factor of 4). Fitted curves are given as solid lines.

The deduced polydispersity indices p (Table II) were used to calculate $2\kappa + \bar{\kappa}$ for the various systems by means of Eq. (4). The same has been done using the macroscopic interfacial tension and the measured mean radii R_m by means of Eq. (5). Both values are given in Table II (below p and γ, respectively) and coincide quite well considering that they were obtained from completely independent measurements. Looking at the obtained values one finds that $2\kappa + \bar{\kappa}$ increases with increasing chain length of the alkyl chain of the surfactant, being about 1 kT for the C_8 surfactants, about 2kT for the C_{10} surfactants, and about 3 kT for $C_{12}E_5$. However, no dependence on the length of the EO head group is observed as, for example, $C_{10}E_4$, $C_{10}E_6$, and $C_{10}E_6$ yield basically identical values. This shows that for the investigated nonionic surfactants, evidently the elasticity of the amphiphilic film is exclusively determined by the length of the alkyl chain and hardly affected at all by the length of the hydrophilic EO head groups. We note, however, that the exact numerical values for the elastic constants depend on the model used for the entropy of mixing.[9]

Finally, it may be observed that Eq. (6), which interrelates the experimentally accessible quantities p, R, and γ, is quite well fulfilled, i.e., the factor W is in the range of 0.6–1.3 kT for all samples investigated (see Table II). This means that the simple relation given by Eq. (6) is a very useful means to predict properties of the corresponding microemulsion.

B. Alkyl amine oxides

In the next step, a series of other nonionic surfactants, the zwitterionic alkyldimethyl amine oxides were investigated. Here the alkyl chain length was varied from dodecyl up to oleyl.

Again SANS measurements were done on samples saturated with D_{22}-decane. The obtained scattering curves are given in Fig. 2. In all cases a relatively marked minimum was observed, which indicates a relatively low polydispersity of the aggregates. The minimum moves to higher q values with decreasing chain length of the surfactant. This means
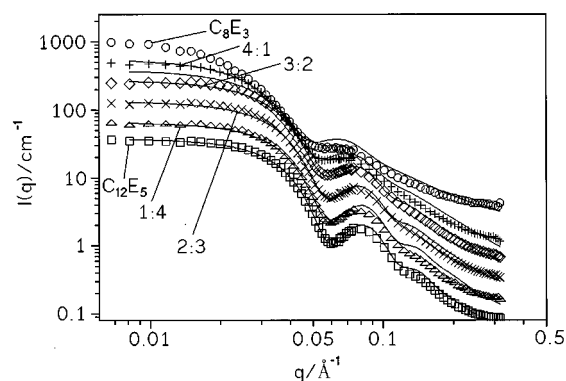
that the microemulsion droplets are larger the longer the alkyl chain of the surfactant, i.e., the longer surfactants are able to solubilize larger amounts of decane.

It is interesting to note that this minimum becomes increasingly more pronounced with increasing chain length of the surfactant, i.e., the microemulsion droplets become less polydisperse. The scattering curves were analyzed with the shell model with sharp boundaries (model 1), which here showed superior results in comparison with those of the diffuse boundaries (model 2). This appears to be reasonable since the amine oxides, in comparison with the polyglycol monoalkylethers C_iE_j, should form a more compact shell, in particular because of its more compact head group, which is not expected to protrude into the aqueous surrounding.[29–31]

From the deduced parameters (Table III), again one can calculate the sum $2\kappa + \bar{\kappa}$ both from the polydispersity index p and from the interfacial tension γ (together with R_m). Again, both values show reasonable agreement and identical trends to those observed for the polyglycol ethers. This means they increase with increasing chain length of the surfactant. In addition, it is found that the parameter W, as defined by Eq. (6), is again always very close to the predicted value of $k \cdot T$.

The only larger deviation is observed for the case of C_{12}DMAO, but this might be explained by the fact that C_{12}DMAO, solubilizes only a fairly small amount of decane (about 0.4 molecules of decane per surfactant molecule). Therefore, it is not any longer a good example for a microemulsion droplet, and the assumption, inherent in all theoretical descriptions, of having a thin surfactant film covering the oil droplet, certainly is not any longer well fulfilled in this case. This might account for the deviations that are observed for the C_{12}DMAO, although it should be noted that these deviations are not really that large, and in general the microemulsion theory appears still to be applicable to the amine oxide systems.
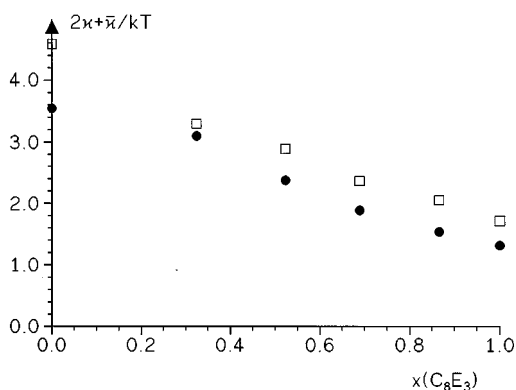
FIG. 5. The sum $2\kappa + \bar{\kappa}$ as deduced from the polydispersity index p as a function of the mole fraction x of C_8E_2 in the surfactant mixture $C_{12}E_5/C_8E_3$ (●: from p; □: from $\gamma \cdot R_m^2$).

C. Dependence on the chain length

In Fig. 3 we have summarized our findings for $2\kappa + \bar{\kappa}$, both for the C_iE_j and the amine oxide surfactants, and they are plotted as a function of the alkyl chain length i. It is very interesting to note that a systematic increase as a function of the chain length is observed and that the values coincide for the different types of surfactants. Evidently the value for $2\kappa + \bar{\kappa}$, is not only independent of the chain length of the EO head groups for the C_iE_j surfactants (as found in Sec. V A), but appears to be quite generally independent of the choice of the head group (at least as long as it is nonionic). The elasticity of the amphiphilic film is dominated by the length of the alkyl chain of the surfactant, i.e., by the thickness of the hydrophobic moiety, and does not depend on the choice of the head group. This means that the effective thickness of the amphiphilic film is just determined by the alkyl chain of the surfactant. It might be noted here that this result also confirms the assumption that the bending constants are mainly determined by the conformational entropy of the flexible hydrocarbon chain, which has been used in the theoretical calculation of the bending moduli with a molecular model.[32]

Now, in general, one can expect the elastic properties of the amphiphilic film to be proportional to its thickness. This thickness may be estimated from the length of the corresponding surfactant molecule. The maximum length l_m of an alkyl chain made up from i carbon atoms can be estimated according to[33]

$$l_m/\text{Å} = 1.5 + 1.265 \cdot i. \tag{8}$$

The thickness l of the surfactant film may be estimated to be this maximum length of the alkyl part of the surfactant molecule plus 2.5 Å for the part of the polar head group that is embedded in this film. Using this value l_m for the thickness of the amphiphilic film, we fitted a power law dependence to our various experimental data for $2\kappa + \bar{\kappa}$ as a function of the alkyl chain length. By doing so we can describe our experimental values for the sum of the elastic constants empirically by the following relation (plotted as a solid line in Fig. 3):

$$(2\kappa + \bar{\kappa})/kT = 4.51 \cdot 10^{-4} \cdot l_m^{2.95}. \tag{9}$$

It is interesting to note that our experimentally determined exponent of 2.95 is very close to the theoretical value of ~ 3 as it is predicted for κ on the basis of an elastic theory that takes into account the conformational statistics of the alkyl chain.[32,34,35] This means that the rigidity of the amphiphilic film is approximately given by a scaling law with the thickness to the power of 3. It might be noted here that such a power dependence is quite generally expected for the bending of a two-dimensional object of certain thickness,[36] and this shows that the surfactant film concerned here should form a compact layer. Our experiments demonstrate that this power dependence not only holds for the mean bending modulus κ but also for the sum $2\kappa + \bar{\kappa}$.

D. Mixtures of surfactants of different alkyl chain length—the system $C_8E_3/C_{12}E_5$

After having investigated the variation of the chain length of the surfactant, a natural extension of our studies is to address the question of what happens if one instead looks at mixtures of surfactants with different alkyl chain length. In order to study such a mixture, we chose the system $C_8E_3/C_{12}E_5$, where from looking at the values for the pure compounds it is clear that the admixture of C_8E_3 to $C_{12}E_5$ will reduce the stiffness of the amphiphilic film.

Here O/W microemulsions formed with decane as oil were studied at 10 °C and all samples were at the emulsification boundary, i.e., just in the two-phase equilibrium with excess oil. SANS measurements (with D_{22}-decane) were done on samples that had a volume fraction of about 8%. The obtained scattering curves are given in Fig. 4, and it can easily be seen from the shift of the minima of the scattering curves that the size of the droplets remains roughly constant, becoming only slightly larger upon increasing the C_8E_3 content. Much more pronounced is the increase of the polydispersity index p (as seen in the curves in the form of a less pronounced bump with increasing C_8E_3 content), which almost doubles from about 0.11 to 0.2.

Again from p, one can directly calculate $2\kappa + \bar{\kappa}$, and one finds that it decreases roughly linearly with the mole fraction of C_8E_3 (Fig. 5). This result might be compared to theoretical calculations[32,37] that predict a more hyperbolic decrease of κ, and in particular a fairly sharp decrease of κ for the admixture of relatively small amounts of the shorter chain surfactant. Of course, we did not observe κ exclusively, but the sum $2\kappa + \bar{\kappa}$, and the same calculations[32] also showed that $\bar{\kappa}$ has a reverse behavior, i.e., a sharp increase for admixture of small amounts of the short chain surfactant, that might compensate for the effect of κ somewhat. This then would explain why we experimentally observe an almost linear relation between $2\kappa + \bar{\kappa}$ and the molar composition of the surfactant mixture.

Furthermore, the interfacial tension γ of corresponding samples was measured and its values are given in Table IV, together with the values for $2\kappa + \bar{\kappa}$, as they can be calculated according to Eq. (4). These values are in good agreement with those obtained from the polydispersity index (always somewhat higher) and are also included in Fig. 5. Finally, it

TABLE IV. Mean radius R_m, polydispersity index p and $2\kappa + \bar{\kappa}$ (as deduced from p), as well as interfacial tension γ and $2\kappa + \bar{\kappa}$ (as deduced from γ) and the factor W [Eq. (5)] for surfactant mixtures of C_8E_3 and $C_{12}E_5$ at 10 °C.

mol % C_8E_3	0	32.4	52.3	68.9	86.6	100
R_m in Å	49.8	50.5	50.7	51.6	54.6	59.2
p	0.111	0.119	0.138	0.158	0.178	0.195
$(2\kappa + \bar{\chi})/kT$	3.54	3.10	2.38	1.89	1.54	1.32
γ in mN/m	0.688	0.467	0.400	0.310	0.235	0.164
$(2\kappa + \bar{\chi})/kT$	4.59	3.30	2.89	2.37	2.06	1.72
W/kT	1.35	1.08	1.26	1.33	1.43	1.41

should be noted that the factor W [compare Eq. (5)] is for all samples relatively close to its theoretically predicted value (Table IV).

VI. CONCLUSIONS

We have investigated the structural parameters (in particular mean radius R and polydispersity index p) of microemulsion droplets as well as their macroscopic interfacial tension γ. These investigations allow for two independent approaches to calculate the sum $2\kappa + \bar{\kappa}$ (with κ: mean bending modulus; $\bar{\kappa}$: Gaussian modulus). For all cases studied, both approaches, i.e., either via the polydispersity index p or the interfacial tension γ, yield rather similar values, thereby proving this method to be quite reliable for the determination of the elastic constants of an amphiphilic film.

In all cases, oil-in-water (O/W) microemulsions were studied with various nonionic surfactants. Both the length of the alkyl chain and the length and type of the polar head groups were varied. The analysis of the experiment data clearly shows that the values deduced for $2\kappa + \bar{\kappa}$ depend almost exclusively on the length of the alkyl chain, and are hardly at all affected by the nature of the head group. This means that for O/W microemulsions of the given type, the elasticity of the amphiphilic film seems to be determined just by the length of the alkyl chain of the surfactant. Since, in turn, this sum $2\kappa + \bar{\kappa}$ also determines the experimentally observable quantities like interfacial tension γ and the size and polydispersity of the corresponding droplets, this means that these quantities are also determined just by the length of the alkyl chain of the surfactant.

Other parameters, like the nature of the polar head group (e.g., the number of EO groups, etc.), have almost no influence, and a former study[9] showed that the nature of the solubilized hydrocarbon also bears no influence on the observed parameters. This means that effectively the properties of a given O/W microemulsion system are controlled by the hydrophobic moiety of the amphiphile.

Finally, it has been shown for the fairly large variety of different surfactant systems investigated here, that the experimentally observable quantities polydispersity index p, maximum radius R_m, and interfacial tension γ are connected by a simple relation [Eq. (6)]. This relation allows the prediction of properties of a given microemulsion system from the other known quantities.

[1] S. A. Safran and L. A. Turkevich, Phys. Rev. Lett. **50**, 1930 (1983).
[2] S. A. Safran, L. A. Turkevich, and P. A. Pincus, J. Phys. **45**, L69 (1984).
[3] D. Andelman, M. E. Cates, D. Roux, and S. A. Safran, J. Chem. Phys. **87**, 7229 (1987).
[4] P. G. de Gennes and C. Taupin, J. Phys. Chem. **86**, 2294 (1982).
[5] S. A. Safran, Phys. Rev. A **43**, 2903 (1991).
[6] S. A. Safran, J. Chem. Phys. **78**, 2073 (1983).
[7] R. Strey, Colloid Polym. Sci. **272**, 1005 (1994).
[8] F. Sicoli and D. Langevin, J. Phys. Chem. **99**, 14, 819 (1995).
[9] M. Gradzielski, D. Langevin, B. Farago, Phys. Rev. E **53**, 3900 (1996).
[10] H. Leitao, A. M. Somoza, M. M. Telo da Gama, T. Sottmann, and R. Strey, J. Chem. Phys. **105**, 2875 (1996).
[11] X.-L. Wu, P. Tong, J. S. Huang, J. Colloid Interface Sci. **148**, 105 (1992).
[12] J. P. Cotton, in *Neutron, X-ray and Light Scattering*, edited by P. Lindner and T. Zemb (Elsevier, New York, 1991), p. 19.
[13] J. L. Cayas, R. S. Schechter, and W. H. Wade, in *Adsorption at Interfaces*, ACS Symposium Series 8, p. 234, Washington, DC, (1975).
[14] M. Burkowsky and C. Marx, Tenside Deterg. **15**, 247 (1978).
[15] B. Vonnegut, Rev. Sci. Instr. **13**, 6 (1942).
[16] T. Sottmann and R. Strey, J. Chem. Phys. (to be published).
[17] K.-V. Schubert and R. Strey, J. Chem. Phys. **95**, 8532 (1991).
[18] K.-V. Schubert, R. Strey, and M. Kahlweit, J. Colloid Interface Sci. **141**, 21 (1991).
[19] W. Helfrich, Z. Naturforsch. C **28**, 693 (1973).
[20] S. A. Safran, in *Structure and Dynamics of Strongly Interacting Colloids and Supramolecular Aggregates in Solution*, edited by S. H. Chen, J. S. Huang, and P. Tartaglia, p. 237, Vol. 369 of NATO Advanced Study Institute, Series C: Mathematical and Physical Sciences (Kluwer, Dordrecht, 1992).
[21] S. T. Milner and S. A. Safran, Phys. Rev. A **36**, 4371 (1987).
[22] J. Meunier and L. T. Lee, Langmuir **7**, 1855 (1991).
[23] M. Borkovec, J. Chem. Phys. **91**, 6268 (1989).
[24] M. Gradzielski, D. Langevin, L. Magid, and R. Strey, J. Phys. Chem. **99**, 13,232 (1995).
[25] N. W. Ashcroft and J. Lekner, Phys. Rev. **145**, 83 (1966).
[26] M. Kahlweit and R. Strey, Angew. Chem. Int. Ed. **24**, 654 (1985).
[27] L. S. Ornstein and F. Zernike, Proc. Ned. Akad. Sci. **17**, 793 (1914).
[28] K. V. Schubert, R. Strey, S. R. Kline, and E. W. Kaler, J. Chem. Phys. **101**, 5343 (1994).
[29] K. A. Dill, D. E. Koppel, R. S. Cantor, J. D. Dill, D. Bendedouch, and S.-H. Chen, Nature **309**, 42 (1984).
[30] B. Cabane, R. Duplessix, and T. Zemb, J. Phys. (Paris) **46**, 2161 (1985).
[31] Y. Chevalier and C. Chachaty, J. Phys. Chem. **89**, 875 (1985).
[32] I. Szleifer, D. Kramer, A. Ben-Shaul, W. M. Gelbart, and S. A. Safran, J. Chem. Phys. **92**, 6800 (1990).
[33] C. Tanford, *The Hydrophobic Effect: Formation of Micelles and Biological Membranes*, 2nd ed. (Wiley, New York, 1980).
[34] I. Szleifer, D. Kramer, A. Ben-Shaul, D. Roux, and W. Gelbart, Phys. Rev. Lett. **60**, 1966 (1988).
[35] C. R. Safinya, E. B. Sirota, D. Roux, and G. S. Smith, Phys. Rev. Lett. **62**, 1134 (1989).
[36] L. D. Landau and E. M. Lifschitz, *Lehrbuch der Theoretischen Physik, Band VII Elastizitätstheorie* (Akademie, Berlin, 1989).
[37] S. May and A. Ben-Shaul, J. Chem. Phys. **103**, 3839 (1995).